POLITECNICO DI TORINO
Repository ISTITUZIONALE

Harmonic analysis and reduction of the scattered field from electrically large cloaked metallic cylinders

Original
Harmonic analysis and reduction of the scattered field from electrically large cloaked metallic cylinders / Cappello, B., Matekovits, L.. - In: APPLIED OPTICS. - ISSN 1559-128X. - 59:12(2020), pp. 3742-3750. [10.1364/AO.387246]

Availability:
This version is available at: 11583/2828472 since: 2020-05-22T11:11:39Z

Publisher:
OSA - The Optical Society

Published
DOI:10.1364/AO.387246

Terms of use:

This article is made available under terms and conditions as specified in the corresponding bibliographic description in the repository

Publisher copyright
Optica Publishing Group (formely OSA) postprint/Author's Accepted Manuscript

"© 2020 Optica Publishing Group. One print or electronic copy may be made for personal use only. Systematic reproduction and distribution, duplication of any material in this paper for a fee or for commercial purposes, or modifications of the content of this paper are prohibited."

(Article begins on next page)

13 October 2026

Harmonic analysis and reduction of the scattered field from electrically large cloaked metallic cylinders

BARBARA CAPPELLO* **AND LADISLAU MATEKOVITS**

Department of Electronics and Telecommunications, Politecnico di Torino, Corso Duca degli Abruzzi 24, 10129 Torino, Italy.
barbara.cappello@polito.it

Abstract: In this paper an analysis of the spectral composition of the scattered field from coated metallic cylinders is performed, focusing particularly on the cloaking of electrically large structures. An expression of the scattering coefficients is derived considering both a dielectric and a metasurface coating. Modelling the metasurface as a surface impedance boundary condition, the surface impedance which annuls one harmonic of the scattered field is formulated in a closed and compact form. Moreover, in the case of cylinders with radius comparable with the wavelength of interest, it is demonstrated that a reduction of the scattering is possible by using a homogeneous metasurface coating which presents a positive surface reactance. In particular, a reduction of the scattering width of 4 dB is achieved for a cylinder radius $a = 0.917\lambda_0$.

© 2020 Optical Society of America

1. Introduction

In last years, metamaterials and metasurfaces have been widely studied [1–4]. Usually, they consist in (quasi-) periodic structures that present equivalent properties that are not present in natural materials, such as for example negative permittivity or permeability [5, 6]. Thanks to their particular characteristics, these materials can be used to control the propagation of waves, and have found different applications in electromagnetics such as absorbers [7, 8], lenses [9, 10], leaky wave antennas [11], etc.

One interesting application of metamaterials is the possibility to use them to cover an object in order to control its scattered field and in particular to cloak the object by strongly reducing its scattering in such a way to not affect the wave propagation in the surrounding environment of the object.

One of the first methods developed to realize a cloaking effect was the so-called Transformation Optics, which is based on the use of strongly anisotropic materials with the aim of controlling the wave propagation and bending it around the object [12]. The principal drawbacks of this technique were the important dimension of the coating structure and the need of a material with an anisotropic permittivity and permeability, which can also assume negative values.

In later years, a different approach based on scattering cancellation was proposed. Both Plasmonic [13] and Mantle Cloaking [14] methods belong to this category. However, while Plasmonic Cloaking is based on the characterization of the coating layer in terms of permittivity ε_r, and still requires a negative value of ε_r, Mantle Cloaking focuses on a formulation of the problem in terms of surface impedance boundary condition. Moreover, it has the advantage of requiring a thin patterned metasurface rather than a bulk 3D metamaterial coating.

For these reasons, many studies in recent years have been focused on the Mantle Cloaking approach. Nevertheless, the cloaking of electrically large objects in terms of wavelength is still challenging. The principal problem in this scenario is represented by the increasing number of harmonics that contributes to the scattered field. In order to overcome this problem, different solutions where proposed such as the use of multiple cloaking layers [15, 16], or the use of

active components inserted in the metasurface [17, 18]. However, in the first case, the coating thickness becomes important with respect to the object dimensions, making the object bulk and heavy; moreover, the design and the manufacturing of the cloaking is more complex; while, in the second case, the cost of fabrication is increased with respect to passive systems also due to the presence of the active elements and of the control network. Other approaches based on an anisiotropic metasurface coat and therefore on the definition of a tensorial surface impedance were also proposed [19, 20].

Therefore, the goal of this paper is to investigate the scattering reduction that can be achieved by using passive, homogeneous and single layered structures, which will be the main focus throughout the paper. In particular, a theoretical analysis of the scattered field of a coated metallic cylinder in terms of harmonic content is performed and the spectral composition of the field is studied for different boundary conditions, namely for a dielectric coated metallic cylinder and for a metasurface cloaked one.

Moreover, considering the cloaked structure, the surface admittance that annuls a specific harmonic of the scattered field is derived in a closed and compact form.

The effects of the surface impedance and of the geometrical and material parameters of the structure are investigated for a real-life configuration with the aim to globally reduce the scattering coefficients and therefore the scattered field. In particular, the possibility to use a homogeneous surface impedance condition to cloak an electrically large object, i.e., with dimensions comparable to the wavelength of interest, is discussed. With this aim, the use of an appropriate dielectric thickness and permittivity and a positive surface reactance is proposed as a possible solution, and it is validated with a numerical analysis.

The paper is structured as follows. In Sec. 2 an analysis of the scattered field from a bare metallic cylinder and from a dielectric coated cylinder is performed. An analytical formulation of the scattering coefficients is given, showing how the thickness and the relative permittivity of the dielectric layer can control the position of the zeros and the maxima of the coefficients. In Sec. 3, a similar analysis is performed for cloaked cylinders, focusing the attention on non-electrically small structures. Moreover, a formulation of the surface impedance which annuls one harmonic of the scattering is derived and compared with previous literature results. Finally in Sec. 4 the theoretical results are validated with a numerical simulation.

2. Metallic and dielectric coated cylinders

The considered structure is composed by an infinite long perfectly electric conductor (PEC) cylinder with radius a, covered by a dielectric layer with thickness t and relative permittivity ε_r, such that the total radius of the cloaked structure is $b = a + t$. On the dielectric, a metasurface is present. Usually this consists of a periodic metallic pattern printed on the dielectric substrate, which is therefore necessary in order to avoid short circuits between the PEC cylinder itself and the metallic loads. In order to analytically study the structure, the metasurface is modelled as a homogeneous surface impedance boundary condition on the dielectric-background interface.

The structure is illuminated by a normally incident homogeneous planewave with electric field polarized along $\hat{z}$, i.e., parallel to the cylinder axis, as represented in Fig. 1.

In order to analyse the problem, the Lorenz-Mie approach is followed [17]. The electric field is expanded in a sum of cylindrical harmonics, and in particular, the scattered field $\mathbf{E}^s$ in the background medium can be written as:

$$\mathbf{E}^s(\rho, \varphi) = \hat{z} E_0 \sum_{n=-\infty}^{\infty} j^{-n} c_n H_n^{(2)}(k_0 \rho) \exp(jn\varphi) \tag{1}$$

where n is the harmonic order, c_n represents the scattering coefficients and therefore the weight of the associated harmonic in the scattering, $H_n^{(2)}$ are the Hankel functions of second order, k_0 is

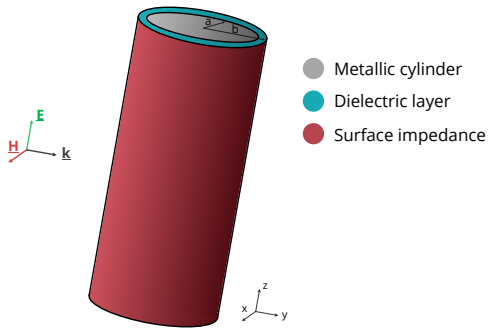

Fig. 1. CAD model of the considered structure. A metallic cylinder is coated by a dielectric layer and a homogeneous surface impedance, and it is illuminated by a TM polarised planewave.

the wavenumber in the background medium, hereafter considered as being vacuum, ρ and φ are the radial and azimuthal cylindrical coordinates.

To understand how the scattered field is modified when a metasurface cover is present on the cylinder, it can be useful to consider, as a first analysis, a bare PEC cylinder and successively a dielectric covered PEC cylinder.

In the bare case, it is known that $c_n = -\frac{J_n(k_0 a)}{H_n^{(2)}(k_0 a)} = -\frac{J_n(k_0 a)}{J_n(k_0 a) - jY_n(k_0 a)}$ [21] (where a is the cylinder radius). Therefore, the modulus of the coefficients c_n is minimum in correspondence of the zeros of the Bessel functions of first kind $J_n(k_0 a)$, while is maximum, and equal to 1, in the zeros of the Neumann functions $Y_n(k_0 a)$.

In Fig. 2 the scattering spectral content of a PEC cylinder is shown for different values of the cylinder radius normalised with respect to the free space wavelength of excitation $a_\lambda = a/\lambda_0$. It can be noticed that: (i) while at low frequency regime only the harmonics with modal index n = 0,1,2 contribute significantly to the scattering and, in particular, the harmonic with order $n = 0$ is dominant; (ii) at higher frequencies a richer harmonic contribution is observed, and a principal harmonic cannot be defined, but different harmonics are equivalently present in the scattered field.

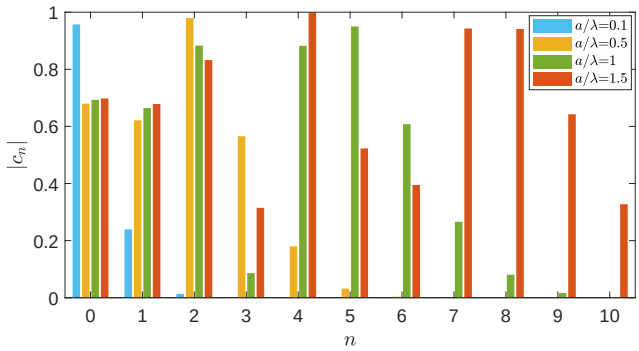

Fig. 2. Absolute value of the scattering coefficients c_n with n = 0:10, for different normalised radius of a bare metallic cylinder.

When the cylinder is covered by a dielectric layer of thickness $t = b - a$ and relative permittivity

ε_r, writing the field inside the dielectric and in the background as a sum of harmonics, and by imposing a continuity boundary condition at the media interfaces, a closed formulation for the scattering coefficients c_n can be obtained as follows (the detailed demonstration is reported in the Appendix):

$$c_n = -\frac{J_n^{'}(k_0 b)p_n - \sqrt{\varepsilon_r} J_n(k_0 b) q_n}{H_n^{'(2)}(k_0 b)p_n - \sqrt{\varepsilon_r} H_n^{(2)}(k_0 b) q_n} \tag{2}$$

where q_n and p_n are the cross products of Bessel functions as denoted in [22], being k_d the wavenumber in the dielectric layer:

$$p_n = J_n(k_d a)Y_n(k_d b) - Y_n(k_d a)J_n(k_d b) \tag{3}$$

$$q_n = J_n(k_d a)Y_n^{'}(k_d b) - Y_n(k_d a)J_n^{'}(k_d b) \tag{4}$$

Remembering that: $H_n^{(2)}(x) = J_n(x) - jY_n(x)$, the coefficients can be written in the form: $c_n = U_n/(U_n - jV_n)$ and, therefore, their absolute value will be maximum and equal to 1 when the condition $V_n = Y_n^{'}(k_0 b)p_n - \sqrt{\varepsilon_r} Y_n(k_0 b) q_n = 0$ is satisfied, while they will annul if $U_n = J_n^{'}(k_0 b)p_n - \sqrt{\varepsilon_r} J_n(k_0 b) q_n = 0$.

Following Eq. (2), Fig. 3 illustrates the absolute value of the first three scattering coefficients $c_{0,1,2}$ versus the normalised cylinder radius a_λ, when a dielectric coated PEC cylinder is considered. In this case the PEC cylinder radius is a = 2 cm, the thickness of the dielectric layer is set to $b = 1.15a$. It can be noticed that by varying the dielectric permittivity and thickness, it is possible to control and to tune the zeros (and the maxima) of different harmonics.

Moreover, since, as seen before, for high values of a_λ three scattering coefficients are not sufficient to describe the scattering, a complete representation of the significant c_n is reported in Fig. 4.

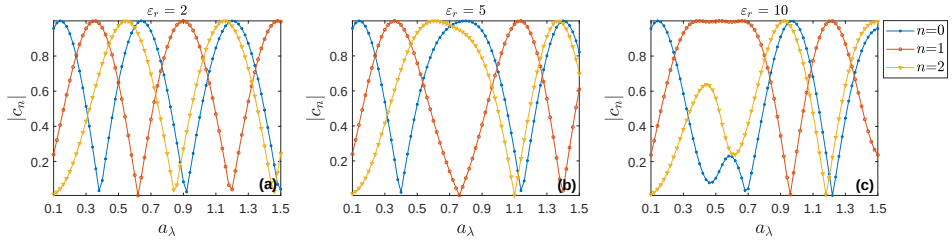

Fig. 3. Absolute value of the first three scattering coefficients c_n with respect to the cylinder normalised radius a_λ, for a dielectric coated metallic cylinder with a = 2 cm, $b = 1.15a$ and ε_r = 2,5,10 (a,b,c).

3. Cloaked cylinders

In this section, the harmonic composition of the scattered field from a metasurface cloaked cylinder is analysed. When the metasurface is present on the boundary of the cloaked cylinder, it can be modelled enforcing an impedance boundary condition that relates the discontinuity of the magnetic field on the object-background interface, i.e., $\rho = b$, with the tangential electric field, such that $\mathbf{E}(b, \varphi) = Z_s \hat{\rho} \times (\mathbf{H}(b^+, \varphi) - \mathbf{H}(b^-, \varphi))$. In this case, losses are neglected, and therefore the surface impedance Z_s is purely imaginary: $Z_s = jX_s = 1/Y_s$.

Following the same procedure as before, considering the field in the two media (dielectric layer and background), and imposing the impedance boundary condition, the expression of the coefficients c_n is derived in terms of the geometrical and materials parameters and the surface impedance value [17]:

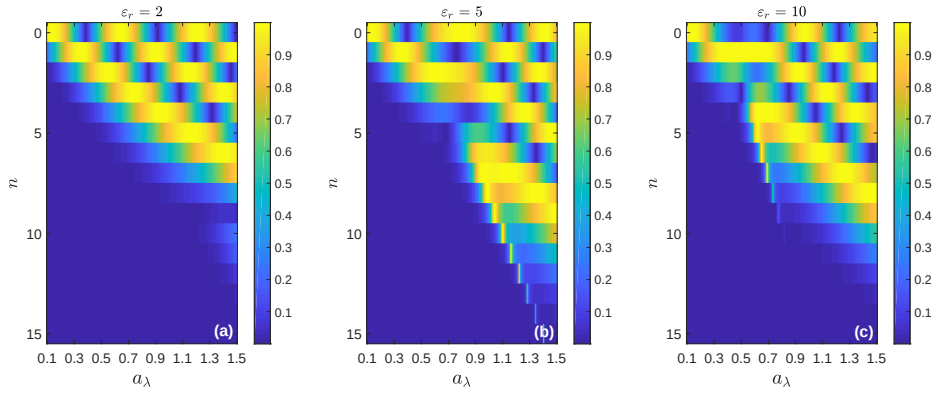

Fig. 4. Absolute value of the scattering coefficients c_n, for $n = 0{:}15$, with respect to the cylinder normalised radius a_λ, for a dielectric coated metallic cylinder with $a = 2$ cm, $b = 1.15a$ and $\varepsilon_r = 2{,}5{,}10$ (a,b,c).

$$c_n = \frac{\begin{vmatrix} J_n(k_d a) & Y_n(k_d a) & 0 \\ J_n(k_d b) & Y_n(k_d b) & J_n(k_0 b) \\ J_n(k_d b) + \frac{k_d}{j\omega\mu} J_n'(k_d b) Z_s & Y_n(k_d b) + \frac{k_d}{j\omega\mu} Y_n'(k_d b) Z_s & \frac{k_0}{j\omega\mu} J_n'(k_0 b) Z_s \end{vmatrix}}{\begin{vmatrix} J_n(k_d a) & Y_n(k_d a) & 0 \\ J_n(k_d b) & Y_n(k_d b) & -H_n^{(2)}(k_0 b) \\ J_n(k_d b) + \frac{k_d}{j\omega\mu} J_n'(k_d b) Z_s & Y_n(k_d b) + \frac{k_d}{j\omega\mu} Y_n'(k_d b) Z_s & -\frac{k_0}{j\omega\mu} H_n^{(2)'}(k_0 b) Z_s \end{vmatrix}} \tag{5}$$

Solving the two determinants it is possible to obtain a closed and compact form to express the coefficients c_n (the detailed derivation is reported in the Appendix):

$$c_n = \frac{-Y_s J_n(k_0 b) p_n - jY_0 J_n'(k_0 b) p_n + jY_0 \sqrt{\varepsilon_r} J_n(k_0 b) q_n}{Y_s H_n^{(2)}(k_0 b) p_n + jY_0 H_n^{(2)'}(k_0 b) p_n - jY_0 \sqrt{\varepsilon_r} H_n^{(2)}(k_0 b) q_n} \tag{6}$$

and therefore:

$$c_n = -\frac{J_n(k_0 b)}{H_n^{(2)}(k_0 b)} \left[\frac{j\tilde{Y}_s - \frac{J_n'(k_0 b)}{J_n(k_0 b)} + \sqrt{\varepsilon_r} \frac{q_n}{p_n}}{j\tilde{Y}_s - \frac{H_n^{(2)'}(k_0 b)}{H_n^{(2)}(k_0 b)} + \sqrt{\varepsilon_r} \frac{q_n}{p_n}} \right] \tag{7}$$

where $\tilde{Y}_s$ is the surface admittance normalized with respect to the background characteristic admittance Y_0, i.e., $\tilde{Y}_s = Y_s / Y_0$.

It can be noticed that in the limit of $Y_s \to \infty$, $c_n = -\frac{J_n(k_0 b)}{H_n^{(2)}(k_0 b)}$. In fact, in this case, the cloaked structure is equivalent to a bare PEC cylinder with radius b.

From Eq. (7) it is possible to compute the normalized surface admittance boundary condition which vanishes a certain coefficient c_n and therefore causes the total annulment of one harmonic:

$$\tilde{Y}_s = -j \left(\frac{J_n'(k_0 b)}{J_n(k_0 b)} - \sqrt{\varepsilon_r} \frac{q_n}{p_n} \right) \tag{8}$$

Interestingly, this result is perfectly coherent with the conclusion of a different approach based on a cylindrical transmission line analysis studied in [23]. In fact, starting from a formulation based on the study of the problem in terms of the contrast of the structure with respect to the background medium, the authors in [23] have described the cloaking phenomena as a cylindrical transmission lines matching problem and derived an expression of $\tilde{Y}_s$:

$$\tilde{Y}_s = -j\frac{J_n'(k_0 b)}{J_n(k_0 b)} + j\sqrt{\varepsilon_r}\left[\frac{H_n^{'(2)}(k_d b) + \gamma(k_d a)H_n^{'(1)}(k_d b)}{H_n^{(2)}(k_d b) + \gamma(k_d a)H_n^{(1)}(k_d b)}\right] \tag{9}$$

where $\gamma(k_d a) = -\frac{H_n^{(2)}(k_d a)}{H_n^{(1)}(k_d a)}$.

If the Hankel functions in Eq. (9) are substituted by their expression in terms of Bessel and Neumann functions, the expression of $\tilde{Y}_s$ as denoted in Eq. (8) is obtained.

From Eq. (8), it can be noticed that with the use of a single homogeneous surface impedance (and therefore a homogeneous metasurface), is it possible to completely cancel one harmonic at one frequency, or to partially reduce different harmonics. In the following, the results on the scattered field of these two approaches will be discussed.

The surface reactances X_s required to suppress the first three harmonics of the coated PEC cylinder are computed using Eq. (8) and are represented in Fig. 5a versus a_λ, which is varied from 0.1 to 1.5. Similarly as before, $b = 1.15a$ and $\varepsilon_r = 10$.

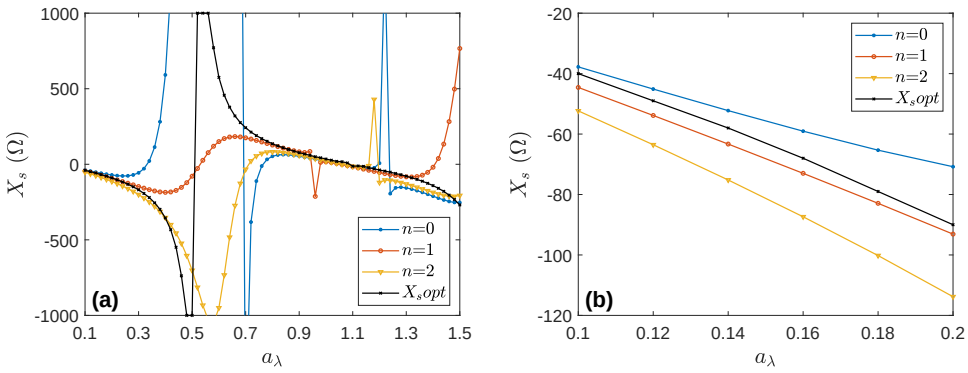

Fig. 5. (a) Surface reactance that cancels the first three harmonics of the scattered field of a cloaked PEC cylinder with respect to the normalised radius a_λ, setting $b = 1.15a$ and $\varepsilon_r = 10$. (b) Detail for low values of a_λ.

As detailed in Fig. 5b, for a normalised radius between 0.1 and 0.2, the surface reactances assume negative values and decrease linearly, in agreement with results in [24, 25]. With the increasing of the normalised radius, resonances are present in correspondence of the normalized radius in which the coefficients of the dielectric coated structure approach the zero.

In order to characterize the cloaking performances, a possibility is to compute the Scattering Width (SW), which is proportional to the ratio of the scattered and incident power:

$$SW = \sigma_{2D} = \lim_{\rho\to\infty} 2\pi\rho\left[\frac{|\mathbf{E}^s|^2}{|\mathbf{E}^i|^2}\right] \tag{10}$$

By substituting in Eq. (10) the scattered field as formulated in Eq. (1) and considering the asymptotic form of $H_n^{(2)}(x)$ for large values of x [22]:

$$\lim_{x\to\infty} H_n^{(2)}(x) = \sqrt{\frac{2}{\pi x}}\exp\left(-j\left(x - \frac{n\pi}{2} - \frac{\pi}{4}\right)\right) \tag{11}$$

and setting $\varphi = 0$, it can be proven [21, 26] that:

$$SW = \frac{2\lambda}{\pi} \left| \sum_{n=-\infty}^{\infty} c_n \right|^2 \tag{12}$$

For small values of the cylinder radius, since the first harmonic is the principal component of the field, as a first approximation, it is sufficient to impose the X_s that annuls the coefficient c_0. However, even in the quasi static limit, it can be proved that the surface reactance which corresponds to the minimum of the SW (from now on referred to as optimum surface reactance X_{opt}) is not equivalent to the one that cancels the dominant harmonics, as illustrated in Fig. 5.

At higher frequencies, a dominant harmonic cannot be identified, therefore, to achieve a minimum of the scattered field, it is necessary to consider the admittance Y_s that corresponds to a minimum of the SW, and consequently to an overall reduction of the coefficients c_n. The optimum surface reactance is reported in Fig. 5 for a = 2 cm, $b = 1.15a$ and $\varepsilon_r = 10$.

In [24] it is proven that for low values of the normalized cylinder radius a_λ, the cloaking metasurface must have a capacitive behaviour for metallic cylinders, and an inductive one for dielectric structures, and it is confirmed in results reported in Fig. 5b.

However, this in no more valid when the cylinder dimension increases. In fact, when the dielectric thickness $t > \lambda_d/4$ where λ_d is the wavelength in the dielectric, the surface impedance changes sign. Therefore, when the static limit is overcome, positive values of X_s should be considered to obtain a scattering reduction. This behaviour can be easily understood considering the problem in terms of transmission lines. In fact, the input impedance of the cloaked structure is equal to the parallel of the surface impedance and the (moved) grounded dielectric layer impedance. To reduce the scattering, this input impedance should be equal to the one of the background medium. However, when the dielectric thickness $t > \lambda_d/4$, the impedance of the grounded dielectric layer, and therefore X_s, changes sign.

This is shown in Fig. 6, which represents the normalised SW of the cloaked cylinder with respect to the bare PEC one, for a value of a_λ varying from 0.1 to 1.5 when X_s is swept from -1000 Ω to 1000 Ω with a step of 1 Ω.

As expected, a decrease of the SW is obtained for a small a_λ and negative impedances. However, it can be noticed that there exists also another part of the response in which the SW is lower with respect to the bare case when the normalised radius increases, which corresponds to positive values of X_s. This periodic behaviour continues with the increasing of the cylinder dimension, even though, it must be underlined that in this case the reduction of the SW will be smaller due to the increasing number of harmonics that constitutes the scattered field.

To further prove this concept, the X_{opt} and the correspondent SW values are shown in Fig. 7 with respect to a_λ considering different properties of the dielectric layer. The SW of the cloaked cylinder are compared to the results obtained for the PEC bare case considering a reference of –3 dB from the PEC results.

As expected, for low a_λ important reductions of the SW are obtained by using a negative reactance value. However, when the cylinder radius is comparable to the wavelength, a reduction of the SW is still possible by using positive values of X_s if appropriate values of b and ε_r are chosen. For example, as detailed in Fig. 7d, a reduction of 3.3 dB of the SW is obtained for a_λ= 1.38, b=1.1a, ε_r = 10 and X_s = 69 Ω.

In literature other approaches to cloak electrically large metallic cylinders based on a single homogeneous metasurface layer have been developed exploiting different techniques. For example the authors in [27] use a low thickness dielectric, such that the cancellation of different harmonics orders requires similar surface impedance values. With this approach a reduction of the SW of 4.8 dB is achieved for $a_\lambda = 0.5$ and of 3.3 dB for $a_\lambda = 0.67$. Here for $a_\lambda = 0.68$ a reduction of 5.4 dB can be achieved, as shown in Fig. 7d. Also in [28] the authors developed a cloak for a cylinder with $a_\lambda = 1.425$ obtaining a reduction of from 1.5 dB to 3 dB of the SW.

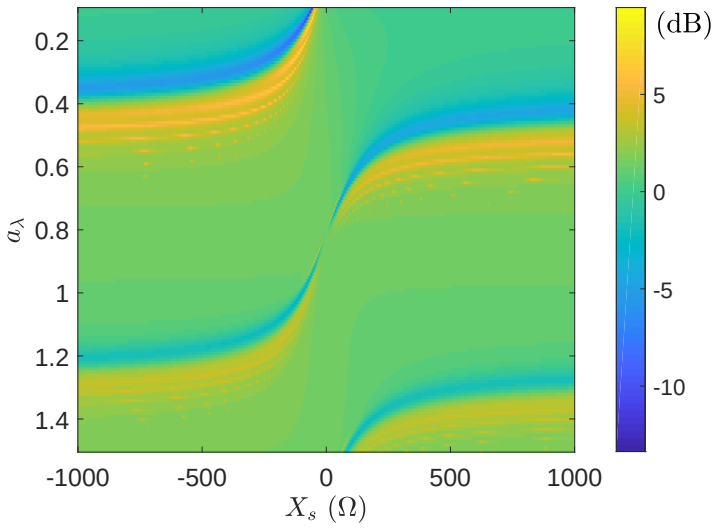

Fig. 6. Difference between the *SW* of the cloaked and bare cylinder with respect to the normalised radius a_λ and the surface reactance X_s, when $b = 1.2a$ and $\varepsilon_r = 10$.

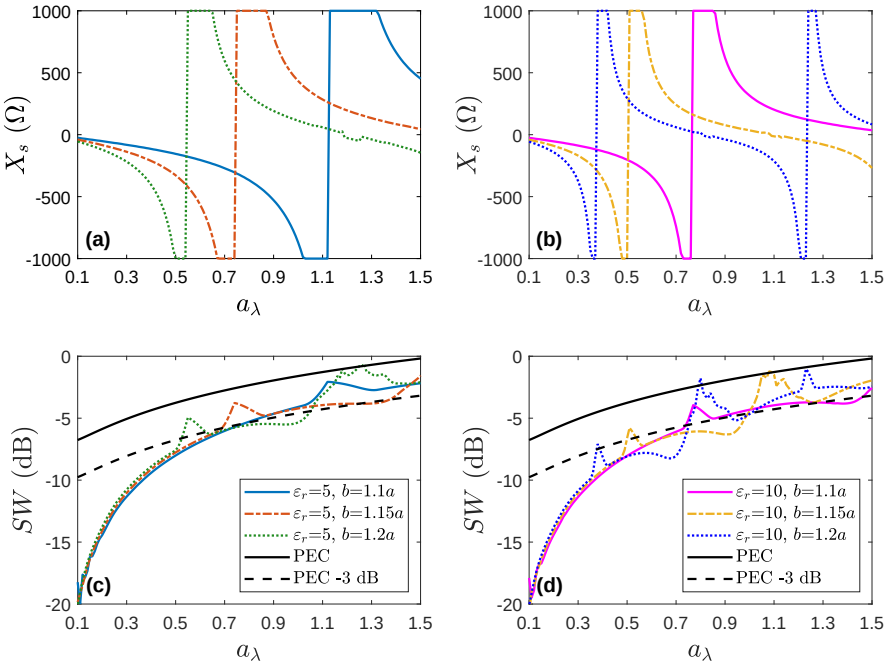

Fig. 7. Optimum surface reactances and correspondent *SW* values for different values of b and ε_r.

4. Numerical simulations

In order to validate the proposed concepts, a specific case is considered and simulated with CST Microwave Studio. The designed structure characteristics are: a = 20 mm, b = 1.15a = 23 mm, ε_r = 10. In order to simulate this structure, the surface impedance is realized with metallic strips parallels to the cylinder axis and printed on the dielectric layer. The thickness of the strips is w = 1.07 mm and unit cell width is D = 4.01 mm as shown in Fig. 8a.

The structure is illuminated by a TM polarised planewave, and to simulate an infinite cylinder, electric boundaries conditions are imposed on the top and bottom of the structure.

The SW computed from the simulated scattered fields of the bare and cloaked cylinder are reported in Fig 8b, showing a reduction of 4 dB at f = 13.75 GHz, correspondent to a normalised radius a_λ = 0.917.

To further validate the model, the full wave simulation results are compared with the theoretical ones by using a semi-analytical approach. Therefore, the dispersion behaviour of the metasurface impedance is numerically evaluated with CST Microwave Studio, by considering a single metasurface unit cell with dimensions DxD and periodic boundary conditions. With the obtained surface impedance values, the scattering coefficients and the scattered field are computed at each frequency point by using Eq. (7) and Eq. (1), respectively. Finally, the SW (which is defined in Fig. 8b as semi-analytical) is evaluated with Eq. (10).

Regarding the bare results, since no metasurface is present, the scattering coefficients, the scattering field and finally the SW are analytically computed. It must be also underlined that to compute the SW a value of ρ = 150 mm is considered in Eq. (10) for both numerical and semi-analytical data. As it can be seen from Fig. 8b the (semi-)analytical and numerical results are in excellent agreement.

Moreover, the simulated scattered electric fields for both the PEC and cloaked cylinder at f = 13.75 GHz are shown in Fig. 9, proving that the scattering is effectively reduced.

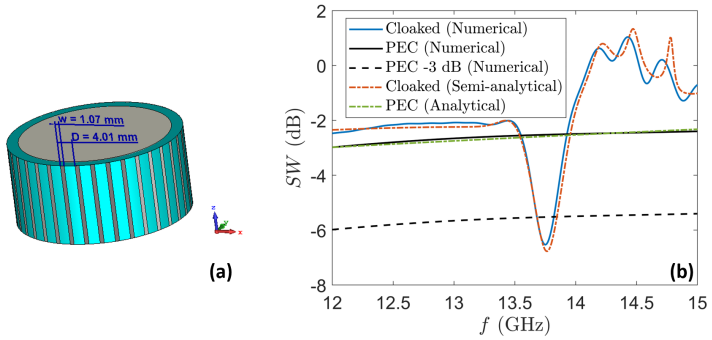

Fig. 8. (a) CAD model of the simulated structure. The cloaking is realised using vertical metallic strips. (b) Simulated SW of the bare and cloaked cylinders and comparison with (semi-)analytical results.

The harmonic analysis of the scattering of the proposed bare and cloaked cylinder is performed at the cloaking frequency f = 13.75 GHz as reported in Fig. 10. First of all, it should be underlined that, since the considered cylinder is not electrically small, the harmonic content cannot be approximated by the single harmonic with modal index n = 0. Moreover, in this case, a clear predominant harmonic is not present. Instead, the higher scattering coefficients correspond to modal indexes n = 4 and n = 1.

Furthermore, the scattering coefficients are compared for different surface reactances, namely X_{opt} = 68 Ω (correspondent to the minimum of the SW), X_s = 48 Ω (which annuls the harmonic

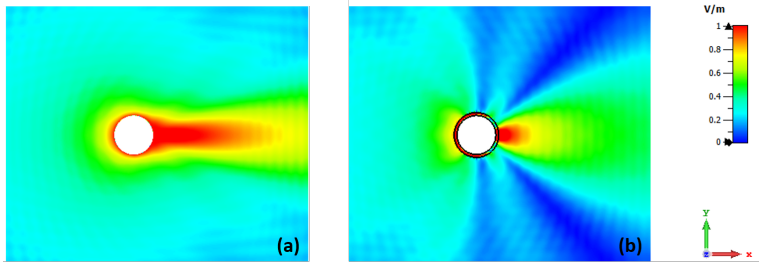

Fig. 9. Simulated scattered electric fields for the bare (a) and the cloaked (b) cylinder at f = 13.75 GHz.

with modal index $n = 0$) and $X_s = 70\ \Omega$ (which annuls the harmonic with modal index $n = 4$). It can be noticed that when $X_{opt} = 68\ \Omega$ is considered, even if some harmonics are increased with respect to the bare case, the average of the scattering coefficients is reduced.

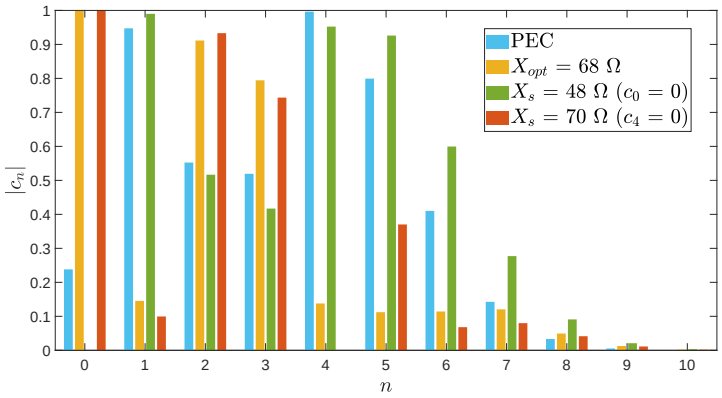

Fig. 10. Absolute value of the scattering coefficients c_n for the proposed bare and cloaked cylinders when different surface impedances are considered.

5. Conclusions

In this paper, an analysis of the scattered field from dielectric coated metallic cylinders and metasurface cloaked cylinders is performed. For both cases, an analytical formulation of the scattering coefficients is derived, discussing how the harmonic composition of the scattering can be controlled by the permittivity and thickness of the dielectric layer. Regarding the cloaked structure, the surface impedance which cancels one harmonic of the scattered field is computed in a closed and compact form. In particular, the use of a homogeneous surface impedance for the cloaking of non-electrically small structure is discussed. In this framework, it is proven that a reduction of the scattered field can be obtained with the use of a positive surface reactance. This could be of particular interest for the analysis and design of more complex structures which use a non homogeneous coat. Finally, the theoretical results are validated by numerical simulations.

Disclosures

The authors declare no conflicts of interest.

References

1. D. R. Smith, W. J. Padilla, D. C. Vier, S. C. Nemat-Nasser, and S. Schultz, "Composite medium with simultaneously negative permeability and permittivity," *Phys. Rev. Lett.* **84**, 4184–4187 (2000).
2. J. B. Pendry, D. Schurig, and D. R. Smith, "Controlling electromagnetic fields," *Science* **312**, 1780–1782 (2006).
3. D. R. Smith, J. J. Mock, A. F. Starr, and D. Schurig, "Gradient index metamaterials," *Phys. Rev. E* **71**, 036609 (2005).
4. W. J. Padilla, D. N. Basov, and D. R. Smith, "Negative refractive index metamaterials," *Mater. Today* **9**, 28 – 35 (2006).
5. R. A. Shelby, D. R. Smith, and S. Schultz, "Experimental verification of a negative index of refraction," *Science* **292**, 77–79 (2001).
6. D. R. Smith, J. B. Pendry, and M. C. K. Wiltshire, "Metamaterials and negative refractive index," *Science* **305**, 788–792 (2004).
7. X. Liu, K. Fan, I. V. Shadrivov, and W. J. Padilla, "Experimental realization of a terahertz all-dielectric metasurface absorber," *Opt. Express* **25**, 191–201 (2017).
8. Y. Yao, R. Shankar, M. A. Kats, Y. Song, J. Kong, M. Loncar, and F. Capasso, "Electrically tunable metasurface perfect absorbers for ultrathin mid-infrared optical modulators," *Nano Lett.* **14**, 6526–6532 (2014). PMID: 25310847.
9. H. Li, G. Wang, J. Liang, X. Gao, H. Hou, and X. Jia, "Single-layer focusing gradient metasurface for ultrathin planar lens antenna application," *IEEE Transactions on Antennas Propag.* **65**, 1452–1457 (2017).
10. A. She, S. Zhang, S. Shian, D. R. Clarke, and F. Capasso, "Large area metalenses: design, characterization, and mass manufacturing," *Opt. Express* **26**, 1573–1585 (2018).
11. E. Abdo-Sánchez, M. Chen, A. Epstein, and G. V. Eleftheriades, "A leaky-wave antenna with controlled radiation using a bianisotropic huygens' metasurface," *IEEE Transactions on Antennas Propag.* **67**, 108–120 (2019).
12. D. Schurig, J. J. Mock, B. J. Justice, S. A. Cummer, J. B. Pendry, A. F. Starr, and D. R. Smith, "Metamaterial electromagnetic cloak at microwave frequencies," *Science* **314**, 977–980 (2006).
13. A. Alù and N. Engheta, "Achieving transparency with plasmonic and metamaterial coatings," *Phys. Rev. E* **72**, 016623 (2005).
14. P.-Y. Chen and A. Alù, "Mantle cloaking using thin patterned metasurfaces," *Phys. Rev. B* **84**, 205110 (2011).
15. A. Abouelsaood, I. Afifi, and I. Eshrah, "Nonresonant and resonant cloaking of an electrically large dielectric spherical object by a multilayer isotropic metamaterial cover," *Appl. Opt.* **54**, 6598–6607 (2015).
16. J. C. Soric, A. Monti, A. Toscano, F. Bilotti, and A. Alù, "Multiband and wideband bilayer mantle cloaks," *IEEE Transactions on Antennas Propag.* **63**, 3235–3240 (2015).
17. S. Liu, H.-X. Xu, H. C. Zhang, and T. J. Cui, "Tunable ultrathin mantle cloak via varactor-diode-loaded metasurface," *Opt. Express* **22**, 13403–13417 (2014).
18. P.-Y. Chen, C. Argyropoulos, and A. Alú, "Broadening the cloaking bandwidth with non-foster metasurfaces." *Phys. review letters* **111 23**, 233001 (2013).
19. Z. H. Jiang and D. H. Werner, "Exploiting metasurface anisotropy for achieving near-perfect low-profile cloaks beyond the quasi-static limit," *J. Phys. D: Appl. Phys.* **46**, 505306 (2013).
20. D.-H. Kwon, "Lossless tensor surface electromagnetic cloaking for large objects in free space," *Phys. Rev. B* **98**, 125137 (2018).
21. C. A. Balanis, *Advanced Engineering Electromagnetics* (John Wiley & Sons, Inc, 1989).
22. I. A. S. M. Abramowitz, *Handbook of mathematical functions, with Formulas, graphs, and mathematical tables* (Dover Publications, New York, 1965).
23. G. Labate, S. K. Podilchak, and L. Matekovits, "Closed-form harmonic contrast control with surface impedance coatings for conductive objects," *Appl. Opt.* **56**, 10055–10059 (2017).
24. Y. R. Padooru, A. B. Yakovlev, P.-Y. Chen, and A. Alù, "Analytical modeling of conformal mantle cloaks for cylindrical objects using sub-wavelength printed and slotted arrays," *J. Appl. Phys.* **112**, 034907 (2012).
25. B. Cappello, G. Labate, and L. Matekovits, "A surface impedance model for a microstrip-line based metasurface," in *2017 International Conference on Electromagnetics in Advanced Applications (ICEAA),* (2017), pp. 429–432.
26. K. Barkeshli, *Advanced electromagnetics and scattering theory* (Springer, 2015).
27. S. Liu, H. C. Zhang, H.-X. Xu, and T. J. Cui, "Nonideal ultrathin mantle cloak for electrically large conducting cylinders," *J. Opt. Soc. Am. A* **31**, 2075–2082 (2014).
28. H. Younesiraad, M. Bemani, and S. Nikmehr, "Scattering suppression and cloak for electrically large objects using cylindrical metasurface based on monolayer and multilayer mantle cloak approach," *IET Microwaves, Antennas Propag.* **13**, 278–285 (2019).

Appendix

A. Computation of scattering coefficients for a dielectric coated PEC cylinder

The electric and magnetic fields in the different media can be written as:

$$\begin{cases} E^{PEC}(\rho,\varphi) = 0 \\ E^{DIEL}(\rho,\varphi) = \hat{z}\sum_{n=-\infty}^{\infty} j^{-n}\left(a_n J_n(k_d\rho) + b_n Y_n(k_d\rho)\right)\exp(jn\varphi) \\ E^{BACK}(\rho,\varphi) = \hat{z}\sum_{n=-\infty}^{\infty} j^{-n}\left(J_n(k_0\rho) + c_n H_n^{(2)}(k_0\rho)\right)\exp(jn\varphi) \end{cases} \tag{13}$$

$$\begin{cases} H^{DIEL}(\rho,\varphi) = \frac{k_d}{j\omega\mu_d}\hat{\varphi}\sum_{n=-\infty}^{\infty} j^{-n}\left(a_n J_n'(k_d\rho) + b_n Y_n'(k_d\rho)\right)\exp(jn\varphi) \\ H^{BACK}(\rho,\varphi) = \frac{k_0}{j\omega\mu_0}\hat{\varphi}\sum_{n=-\infty}^{\infty} j^{-n}\left(J_n'(k_0\rho) + c_n H_n^{'(2)}(k_0\rho)\right)\exp(jn\varphi) \end{cases} \tag{14}$$

where PEC, $DIEL$ and $BACK$ refer to the perfect conducting cylinder, its dielectric coating, and to the background medium, respectively. J_n, Y_n and $H_n^{(2)}$ are the Bessel, Neumann and Hankel functions, a_n, b_n, c_n are unknown coefficients, n is the harmonic order, k_0 and k_d are the background and dielectric wavenumbers, μ_0 and μ_d are the background and dielectric permeability, ρ and φ are the radial and azimuthal cylindrical coordinates.

By imposing the continuity boundary conditions at the media interface, the following system of equations is obtained:

$$\begin{cases} a_n J_n(k_d a) + b_n Y_n(k_d a) = 0 \\ a_n J_n(k_d b) + b_n Y_n(k_d b) = J_n(k_0 b) + c_n H_n^{(2)}(k_0 b) \\ \frac{k_d}{j\omega\mu_d}\left(a_n J_n'(k_d b) + b_n Y_n'(k_d b)\right) = \frac{k_0}{j\omega\mu_0}\left(J_n'(k_0 b) + c_n H_n^{'(2)}(k_0 b)\right) \end{cases} \tag{15}$$

For simplicity, the permeability in the dielectric layer is considered equal to the one in the background medium so that $\mu_d = \mu_0 = \mu$.

The system can be written in matrix form:

$$\begin{bmatrix} J_n(k_d a) & Y_n(k_d a) & 0 \\ J_n(k_d b) & Y_n(k_d b) & -H_n^{(2)}(k_0 b) \\ \frac{k_d}{j\omega\mu}J_n'(k_d b) & \frac{k_d}{j\omega\mu}Y_n'(k_d b) & -\frac{k_0}{j\omega\mu}H_n^{'(2)}(k_0 b) \end{bmatrix} \begin{bmatrix} a_n \\ b_n \\ c_n \end{bmatrix} = \begin{bmatrix} 0 \\ J_n(k_0 b) \\ \frac{k_0}{j\omega\mu}J_n'(k_0 b) \end{bmatrix} \tag{16}$$

Therefore, the scattering coefficients c_n can be obtained as:

$$c_n = \frac{\det(C)}{\det(A)} \tag{17}$$

where:

$$A = \begin{bmatrix} J_n(k_d a) & Y_n(k_d a) & 0 \\ J_n(k_d b) & Y_n(k_d b) & -H_n^{(2)}(k_0 b) \\ \frac{k_d}{j\omega\mu}J_n'(k_d b) & \frac{k_d}{j\omega\mu}Y_n'(k_d b) & -\frac{k_0}{j\omega\mu}H_n^{'(2)}(k_0 b) \end{bmatrix} \tag{18}$$

$$C = \begin{bmatrix} J_n(k_d a) & Y_n(k_d a) & 0 \\ J_n(k_d b) & Y_n(k_d b) & J_n(k_0 b) \\ \frac{k_d}{j\omega\mu}J_n'(k_d b) & \frac{k_d}{j\omega\mu}Y_n'(k_d b) & \frac{k_0}{j\omega\mu}J_n'(k_0 b) \end{bmatrix} \tag{19}$$

Solving the determinants:

$$\begin{aligned} \det(C) = {} & J_n(k_d a)\left(\frac{k_0}{j\omega\mu}Y_n(k_d b)J_n'(k_0 b) - \frac{k_d}{j\omega\mu}J_n(k_0 b)Y_n'(k_d b)\right) \\ & -Y_n(k_d a)\left(\frac{k_0}{j\omega\mu}J_n(k_d b)J_n'(k_0 b) - \frac{k_d}{j\omega\mu}J_n(k_0 b)J_n'(k_d b)\right) \end{aligned} \tag{20}$$

Setting: $k_0/(j\omega\mu) = -jY_0 = k$ and $k_d/(j\omega\mu) = k\sqrt{\varepsilon_r}$,

$$\begin{aligned}\det(C) = kJ_n(k_d a)Y_n(k_d b)J_n^{'}(k_0 b) - k\sqrt{\varepsilon_r}J_n(k_d a)J_n(k_0 b)Y_n^{'}(k_d b)\\ -kY_n(k_d a)J_n(k_d b)J_n^{'}(k_0 b) + k\sqrt{\varepsilon_r}Y_n(k_d a)J_n(k_0 b)J_n^{'}(k_d b)\end{aligned} \tag{21}$$

$$\begin{aligned}\det(C) = kJ_n^{'}(k_0 b)\left(J_n(k_d a)Y_n(k_d b) - Y_n(k_d a)J_n(k_d b)\right)\\ -k\sqrt{\varepsilon_r}J_n(k_0 b)\left(J_n(k_d a)Y_n^{'}(k_d b) - Y_n(k_d a)J_n^{'}(k_d b)\right)\end{aligned} \tag{22}$$

Defining the cross products of Bessel functions, q_n and p_n as in Eq. (3) and Eq. (4), it is obtained:

$$\det(C) = kJ_n^{'}(k_0 b)p_n - k\sqrt{\varepsilon_r}J_n(k_0 b)q_n \tag{23}$$

Similarly,

$$\det(A) = -kH_n^{'(2)}(k_0 b)p_n + k\sqrt{\varepsilon_r}H_n^{(2)}(k_0 b)q_n \tag{24}$$

Therefore, the scattering coefficients c_n are:

$$c_n = -\frac{J_n^{'}(k_0 b)p_n - \sqrt{\varepsilon_r}J_n(k_0 b)q_n}{H_n^{'(2)}(k_0 b)p_n - \sqrt{\varepsilon_r}H_n^{(2)}(k_0 b)q_n} \tag{25}$$

B. Computation of scattering coefficients for a cloaked PEC cylinder

Similarly to previous case, it is possible expand the field in a sum of harmonics and to consider the boundary conditions at the media interface. In this case, the last equation of Eq. (15) is modified to take into account the surface impedance Z_s, that relates the discontinuity of the magnetic field at the dielectric-background interface with the tangential electric field, such that:

$$\begin{aligned}a_n J_n(k_d b) + b_n Y_n(k_d b) = Z_s\frac{k_0}{j\omega\mu_0}\left(J_n^{'}(k_0 b) + c_n H_n^{'(2)}(k_0 b)\right)\\ -Z_s\frac{k_d}{j\omega\mu_d}\left(a_n J_n^{'}(k_d b) + b_n Y_n^{'}(k_d b)\right)\end{aligned} \tag{26}$$

Following the same procedure of previous case (and considering $\mu_d = \mu_0 = \mu$):

$$c_n = \frac{\det(C^{'})}{\det(A^{'})} \tag{27}$$

where:

$$A^{'} = \begin{bmatrix} J_n(k_d a) & Y_n(k_d a) & 0 \\ J_n(k_d b) & Y_n(k_d b) & -H_n^{(2)}(k_0 b) \\ J_n(k_d b) + \frac{k_d}{j\omega\mu}J_n^{'}(k_d b)Z_s & Y_n(k_d b) + \frac{k_d}{j\omega\mu}Y_n^{'}(k_d b)Z_s & -Z_s\frac{k_0}{j\omega\mu}H_n^{'(2)}(k_0 b) \end{bmatrix} \tag{28}$$

$$C^{'} = \begin{bmatrix} J_n(k_d a) & Y_n(k_d a) & 0 \\ J_n(k_d b) & Y_n(k_d b) & J_n(k_0 b) \\ J_n(k_d b) + \frac{k_d}{j\omega\mu}J_n^{'}(k_d b)Z_s & Y_n(k_d b) + \frac{k_d}{j\omega\mu}Y_n^{'}(k_d b)Z_s & Z_s\frac{k_0}{j\omega\mu}J_n^{'}(k_0 b) \end{bmatrix} \tag{29}$$

Therefore:

$$\begin{aligned}\det(C^{'}) = J_n(k_d a)\left(\frac{k_0}{j\omega\mu}Y_n(k_d b)J_n^{'}(k_0 b)Z_s - J_n(k_0 b)Y_n(k_d b) - \frac{k_d}{j\omega\mu}J_n(k_0 b)Y_n^{'}(k_d b)Z_s\right)\\ -Y_n(k_d a)\left(\frac{k_0}{j\omega\mu}J_n(k_d b)J_n^{'}(k_0 b)Z_s - J_n(k_0 b)J_n(k_d b) - \frac{k_d}{j\omega\mu}J_n(k_0 b)J_n^{'}(k_d b)Z_s\right)\end{aligned} \tag{30}$$

Introducing the variables k, p_n, q_n as previously defined, one gets:

$$\det(C^{'}) = -p_n J_n(k_0 b) + k Z_s p_n J_n^{'}(k_0 b) - k\sqrt{\varepsilon_r} Z_s q_n J_n(k_0 b) \tag{31}$$

The determinant of $A^{'}$ can be derived from $\det(C^{'})$ by substituting $J_n(k_0 b)$ with $-H_n^{(2)}(k_0 b)$:

$$\det(A^{'}) = p_n H_n^{(2)}(k_0 b) - k Z_s p_n H_n^{'(2)}(k_0 b) + k\sqrt{\varepsilon_r} Z_s q_n H_n^{(2)}(k_0 b) \tag{32}$$

so that:

$$c_n = \frac{-p_n J_n(k_0 b) + k Z_s p_n J_n^{'}(k_0 b) - k\sqrt{\varepsilon_r} Z_s q_n J_n(k_0 b)}{p_n H_n^{(2)}(k_0 b) - k Z_s p_n H_n^{'(2)}(k_0 b) + k\sqrt{\varepsilon_r} Z_s q_n H_n^{(2)}(k_0 b)} \tag{33}$$

Substituting $k = -jY_0$ and dividing by $Z_s = 1/Y_s$:

$$c_n = \frac{-Y_s p_n J_n(k_0 b) - jY_0 p_n J_n^{'}(k_0 b) + jY_0\sqrt{\varepsilon_r} q_n J_n(k_0 b)}{Y_s p_n H_n^{(2)}(k_0 b) + jY_0 p_n H_n^{'(2)}(k_0 b) - jY_0\sqrt{\varepsilon_r} q_n H_n^{(2)}(k_0 b)} \tag{34}$$

which can be written as:

$$c_n = \frac{-J_n(k_0 b)}{H_n^{(2)}(k_0 b)} \left[\frac{j\tilde{Y}_s - \frac{J_n^{'}(k_0 b)}{J_n(k_0 b)} + \sqrt{\varepsilon_r}\frac{q_n}{p_n}}{j\tilde{Y}_s - \frac{H_n^{'(2)}(k_0 b)}{H_n^{(2)}(k_0 b)} + \sqrt{\varepsilon_r}\frac{q_n}{p_n}} \right] \tag{35}$$